

Original Research

LINC01311 exerts an inhibitory effect in thyroid cancer progression by targeting the miR-146b-5p/IMPA2 axis

Mengjiang Liu, Linghui Zhang, Juping Hu, Chong Yan, Yi Zhang, Zhaodan Yan*

Department of Endocrinology, Hubei NO.3 People's Hospital of Jiangnan University, No. 26, Zhongshan Avenue, Qiaokou District, Wuhan, Hubei 430033, China

ARTICLE INFO

Keywords:

Thyroid cancer
LINC01311
miR-146b-5p
IMPA2
Migration
Proliferation

ABSTRACT

Background: A growing body of research suggests that long non-coding RNA (lncRNA) play an important role during the tumorigenesis and progression of cancers, including thyroid cancer (TC). Herein, we intended to uncover the role and mechanisms of LINC01311 in TC.

Methods: The relative LINC01311, miR-146b-5p, and IMPA2 expressions were quantified by subjecting TC cells and tissues to western blotting and RT-qPCR. CCK-8 and scratch-wound healing assays were carried out for the evaluation of the proliferation and migration of TC cells. The apoptosis was evaluated by flow cytometry assay and western blotting of Bax and Bcl-2 proteins. Xenograft tumor model was also used to study how LINC01311 functions during TC cell growth. Luciferase reporter and RNA immunoprecipitation (RIP) assays were performed to ascertain miR-146b-5p's interactions with LINC01311 and IMPA2 3'UTR.

Results: The TC cells and tissues exhibited a downregulation of LINC01311 and IMPA2 and an upregulation of miR-146b-5p. LINC01311 overexpression retarded TC cell growth *in vitro* as well as *in vivo*. The luciferase reporter and RIP assays verified that miR-146b-5p recognizes LINC01311 and IMPA2 3'UTR by base pairing. LINC01311 overexpression could counteract the oncogenic effect of miR-146b-5p *in vitro*. Moreover, IMPA2 upregulation could offset the tumor-promoting effect of miR-146b-5p.

Conclusion: LINC01311-mediated inhibition of TC cell growth was achieved by targeting the miR-146b-5p/IMPA2 axis. These findings support that targeting the LINC01311/miR-146b-5p/IMPA2 axis may be a promising approach against TC progression.

Introduction

Thyroid cancer (TC) remains a predominant neoplasm in the endocrine system. TC has had a continuous increase in occurrence for decades, which has declined recently [1]. The progress in multimodal TC treatments has all achieved relatively low mortality rates [2]. In spite of that, TC still comprises about 3% of juvenile cancers [3]. Currently, over diagnosis might be the main reason for the high occurrence, creating a significant medical need for the exploration of possible therapeutic targets. Given these facts, it is crucial to investigate the mechanism behind TC progression.

Long non-coding RNA (lncRNA) is a subfamily of non-coding RNAs with over 200 nt [4]. lncRNA is highly abundant in the human genome, yet it was initially regarded as a transcription byproduct with no bio-function [5]. Recent evidence has underscored the biological importance of lncRNAs. This is due to the increasing exploration of their transcriptional and post-transcriptional regulatory functions, which are

well-established mechanisms that may favor oncogenic drivers or suppressors [6]. During the malignant progression of TC, an increasing number of lncRNAs have been reported to act either as tumor-suppressors or tumor-promoters [7]. For instance, lncRNA XIST evokes the oncogenic PI3K-AKT signaling to facilitate TC progression [8]. lncRNA TUG1 benefits epithelial-mesenchymal transition, which has been linked to the metastatic and invasive properties of TC cells [9]. The oncogenic role of lncRNA RNAMALAT1 is triggered by increasing the expression of myelocytomatosis (MYC), which is a driver of TC cell proliferation [10]. LINC01311 is a novel lncRNA recently reported to be interfering with Alzheimer's disease via epigenetic regulation [11]. However, its role in TC remains obscure.

Reportedly, lncRNA functions as a sponge of microRNA (miRNA), thereby releasing the target gene expressions from miRNA suppression [12]. lncRNA XIST sponges miR-34a and upregulates the expression of hepatocyte growth factor receptor (MRT), thus facilitating TC progression [8]. Furthermore, lncRNA-MIAT serves as miR-150-5p's ceRNA

* Corresponding author.

E-mail address: zhaodanyan3@163.com (Z. Yan).

(competing endogenous RNA) to boost EZH2 expression, thereby favoring oncogenicity during TC progression. The ceRNA activity of LINC01311 to miR-146a-5p has also been described in Alzheimer's disease [11]. Hence, aside from evaluating the function of LINC01311 *in vitro* and *in vivo*, our subsequent mechanistic exploration was also conducted, which aimed to find the miRNA epigenetically silenced by LINC01311. Our bioinformatics analysis revealed that LINC01311 preferentially binds with miR-146b-5p and its tumorigenic role in TC piqued our curiosity [13–16].

Therefore, we investigated the ceRNA activity of LINC01311 with miR-146a-5p during TC malignancy. We are hopeful that our present research may help identify new targets for the treatment of TC.

Methods

Tissue specimens

Twenty-eight [28] pairs of tumoral and noncancerous tissues were surgically obtained from individuals suffering from TC. Each patient submitted a written informed consent. None of the patients underwent neoadjuvant chemotherapy, chemoradiotherapy, or any therapy before the surgical resection. Specimens were sent for pathologic confirmation and were stored at -80°C after snap-freezing for the next assays. Our hospital granted ethical approval to this study.

Cell culture

Normal human primary thyroid follicular epithelial cell line (Nythy-ori3–1) and one of the TC cell lines (TPC-1) were purchased from Millipore (Sigma, USA). Two other TC cell lines (KTC-1 and SW579) were from the Cell Bank of Typical Culture Preservation Committee of the Chinese Academy of Sciences (Shanghai, China). The fourth TC cell line (BCPAP) was from the DSMZ-German Collection of Microorganisms and Cell Cultures (GmbH Germany). BCPAP, KTC-1, TPC-1, and Nythy-ori3–1 were maintained in RPMI 1640 Medium (ThermoFisher, USA) while the SW579 cells were kept in DMEM (ThermoFisher, USA). All cells were grown in an incubator (95% air, 5% CO_2 ; 37°C). While the cells were being cultivated, 1% Penicillin-Streptomycin Solution (ThermoFisher, USA) and 10% FBS (ThermoFisher, USA) were added to the medium.

Cell transfection and infection

MiR-146b-5p mimic or mimic-NC, pcDNA-IMPA2 vectors (IMPA2-OE), and the empty vectors (Empty vector) were obtained from Gema, Shanghai, China. These products were introduced into KTC-1 and TPC-1 cells with the aid of Lipofectamine 2000 reagent (Invitrogen, USA). Forty-eight hours later, the transfection efficiency was ascertained by means of RT-qPCR.

For LINC01311 overexpression, empty plasmids and lentiviral particles harboring LINC01311 cDNA for LINC01311 ectopic expression were purchased from Guangzhou Yunzhou, Biological Technology Co. Ltd, China. The prepared lentiviral vectors were used to infect KTC-1 and TPC-1 cells before a 4-week puromycin maintenance. The survivals were propagated and subjected to RT-qPCR analysis.

RT-qPCR assay

A Total RNA Extraction Kit (Solarbio, China) was utilized to extract total RNA from cells and tissues. PrimeScript RT reagent Kit (Takara, Japan) and One step miRNA RT kit (Haigene, China) were employed for the reverse transcription of 1 μg RNA to cDNA. The cDNA was then amplified and quantified in a Bio-Rad iQ5 Real-Time System with the aid of a Fast SYBR Green Master Mix (Applied Biosystems, USA). The following thermal cycling conditions were used for qPCR: initial denaturation for 5 min at 95°C , followed by 40 cycles of denaturation for 10 s

Table 1

The sequences of the primers in this study.

| Primer | Sequences |
|-------------|--|
| miR-146b-5p | Forward: 5'-TGACCCATCCTGGGCCCTCAA-3' Reverse: 5'-CCAGTGGGCAAGATGTGGGCC-3' |
| IMPA2 | Forward: 5'-TAAGCAGCTAGCATGAAGCCGAGCGGC-3' Reverse: 5'-TGTTTAGAATTCTCACTTCTCATCATCCCGC-3' |
| GAPDH | Forward: 5'-CTGGGCTACACTGAGCACC-3' Reverse: 5'-AAGTGG TCGTTGAGGGCAATG-3' |
| U6 | Forward: 5'-TGCGGGTGCTCGCTTCGGCAGC-3' Reverse: 5'-GGATCCGACGGGTGGTCTTCTCAGA-3' |

at 95°C and amplification/extension for 30 s at 60°C , and one cycle of melt curve analysis according to the instrument's guidelines. GAPDH (for LINC01311 and IMPA2) or U6 (for miR-146b-5p) were adopted to normalize the data with $2^{-\Delta\Delta\text{Ct}}$. Table 1 presents all primers used.

Western blot

The cells were harvested 48 h after transfection and lysed with RIPA buffer (ThermoFisher, USA). After centrifugation (10,000 g at 4°C for 10 min), the concentration of the protein in the resulting supernatant was determined using a BCA Protein Assay Reagent kit (Pierce, USA). Afterward, 20 μg protein samples were resolved on a 10% SDS-PAGE gel before being transferred to PVDF membranes. Each membrane was subsequently blocked with 5% skim milk powder at room temperature for 30 min. Next, the membranes were exposed to diluted specific primary antibodies at 4°C overnight. Thereafter, horseradish peroxidase-conjugated goat anti-rabbit or goat anti-mouse antibodies (Sigma-Aldrich, USA) were added to the membranes at room temperature for 3 h. Finally, a Pierce ECL Western Blotting Substrate was utilized for the visualization of the bands and the same were photographed on a GelDoc XR+ system (Bio-Rad, USA). The antibodies used are as follows: anti-Bcl-2 antibodies (Cat#: 13–8800; 1:10,000; ThermoFisher, USA), anti-Bax antibodies (Cat#: MA5–14,003; 1:10,000; ThermoFisher, USA), anti-IMPA2 antibodies (Cat#: ab256410; 1:10,000; Abcam, USA), anti-GAPDH antibodies (Cat#: ab99252; 1:10,000; Abcam, USA), anti-mouse HRP secondary antibody (Cat#:31,430,1:1000, Invitrogen, USA), and anti-goat HRP secondary antibody (Cat#:31,402,1:1000, Invitrogen, USA).

Flow cytometry

Apoptosis was evaluated by flow cytometry assay with the help of an FITC Annexin V Apoptosis Kit (abcam, USA). TC cells (5×10^5), with or without LINC01311-OE transfection, were incubated at room temperature with 100 μl of 1 \times binding buffer supplemented with 5 μl of propidium iodide solution and 5 μl of FITC Annexin V. Finally, a BD Biosciences flow cytometer was utilized in analyzing the cells.

In vitro proliferation assay

The CCK-8 kit (Sigma, USA) was used to assess TC cell proliferation *in vitro*. In brief, transfected TC cells (2×10^3 cells/well) were seeded into 96-well culture plates and subjected to 24-h, 48-h, and 72-h incubation. Next, 10 μL of CCK-8 reagent was added to each well and incubated for 3 h. Finally, each well was measured for absorbance (OD) at 450 nm with a microplate reader (Promega, USA).

In the vitro migration assay

A scratch wound healing assay was carried out to evaluate cellular migration. TC cells (5×10^3 cells/well) were inoculated into 6-well plates. Upon reaching 95% confluence, linear scratch wounds were created on the cell monolayers using 200 μL pipette tips. The scratched cells were removed, and the plates were maintained in a serum-free

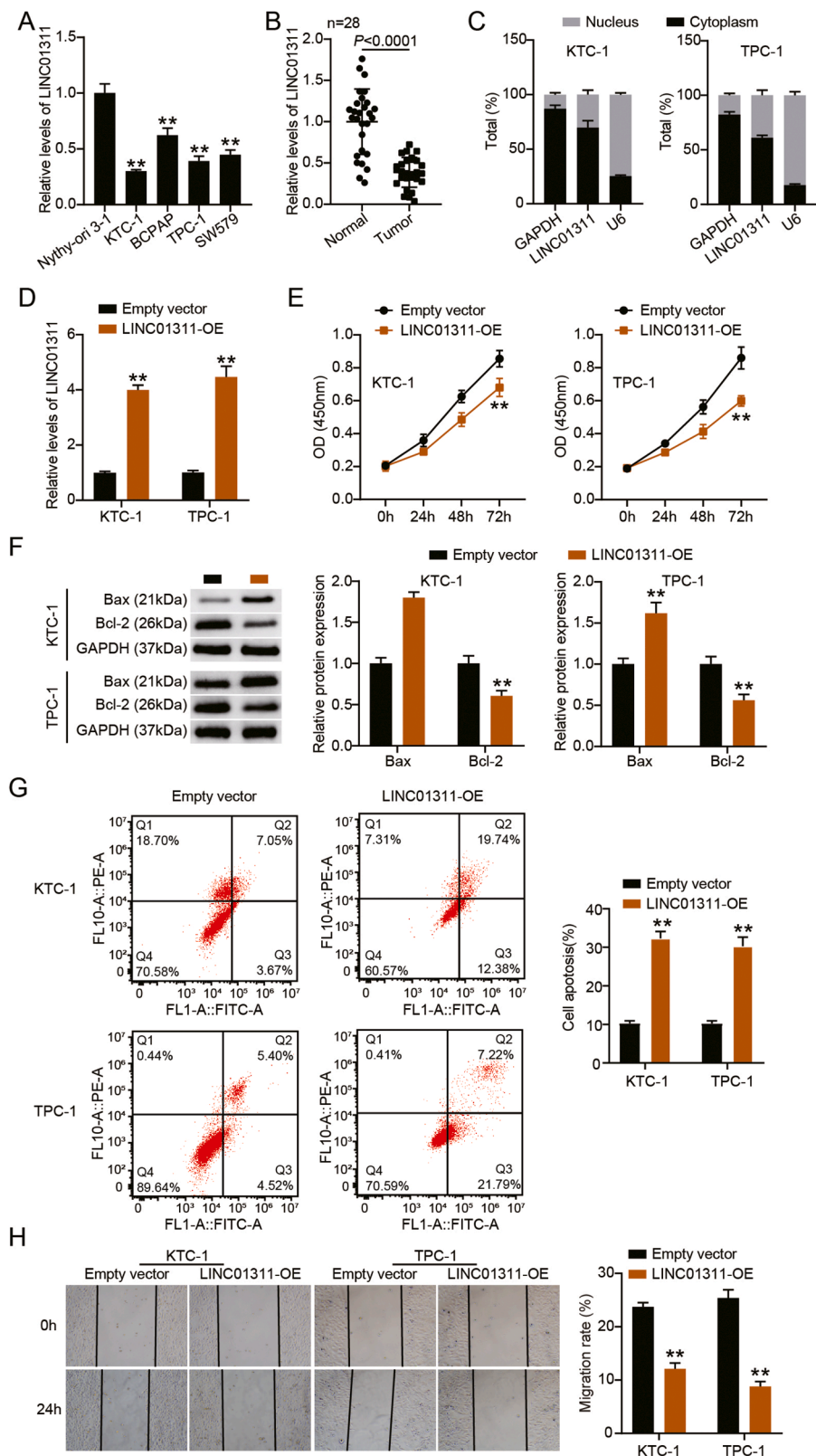


Fig. 1. LINC01311 overexpression suppresses TC cell growth in vitro. (A) RT-qPCR analysis of LINC01311 in TC cells (KTC-1, BCPAP, TPC-1, and SW579) and normal cells (Nythy-ori3-1). [** $P < 0.001$ vs. Nythy-ori3-1; $n = 3$ /group; Dunnett's post hoc test]. (B) RT-qPCR analysis of LINC01311 in TC tissues and normal tissues [** $P < 0.0001$ vs. normal tissues; $n = 28$ /group; Welch's t -test]. (C) LINC01311 localization within the nucleus and the cytoplasm of TC cells was tested by RT-qPCR. (D) RT-qPCR analysis of LINC01311 expression in KTC-1 and TPC-1 cells transfected with Empty vectors or LINC01311-overexpressing vectors (LINC01311-OE). (E) CCK-8 assessment of TC cells transfected with Empty vectors or LINC01311-OE. (F) Western blotting analysis of the expressions of Bcl-2 and Bax in TC cells carrying Empty vectors or LINC01311-OE. (G) Cell apoptosis of TC cells transfected with Empty vectors or LINC01311-OE was examined by Annexin V-FITC/PI-labeled flow cytometry. (H) Scratch wound-healing assay transfected TC cells carrying Empty vectors or LINC01311-OE. [D to H: ** $P < 0.001$ vs. Empty vector; $n = 3$ /group; Student's t -test].

culture medium for 24 h. Photographs of the plates were taken at 0 h and 24 h.

Luciferase reporter assay

The putative binding sequences of LINC01311 and IMPA2 3'UTR

were amplified and inserted into psi-CHECK2TM vectors (Promega, USA) to construct the LINC01311 wild-type (WT) and IMPA2 3'UTR WT luciferase vectors. The corresponding mutant (MUT) vectors were also produced. KTC-1 and TPC-1 cells were transfected with a combination of one of the developed vectors and either a miR-NC or miR-146b-5p mimic. Forty-eight hours post-transfection, the luciferase activities

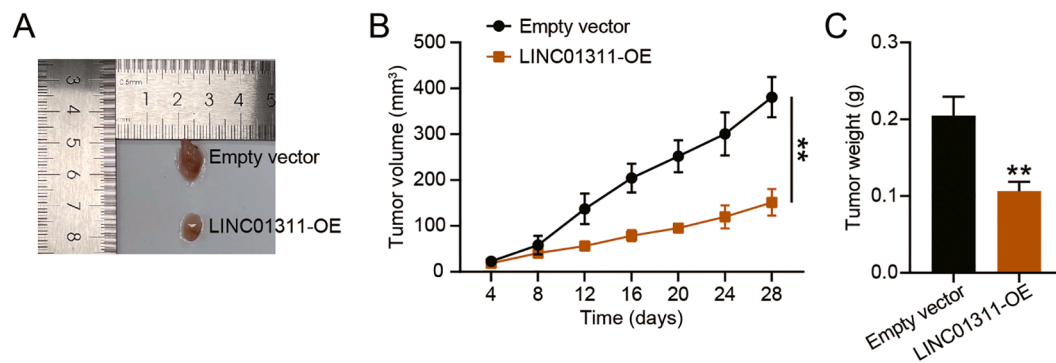


Fig. 2. LINC01311 overexpression restrains TC tumor cell growth *in vivo*. Four to five-week-old BALB/C nude mice were subcutaneously injected with KTC-1 cells infected with lentiviral particles carrying LINC01311 or empty plasmids. Tumor sizes were monitored once every four days. Twenty-eight days later, the mice were euthanized by CO₂ inhalation, and the tumor weight was recorded upon the excision of the xenograft tumors. (A) Representative photograph of xenograft tumors in LINC01311-OE and empty vector groups. (B) Tumor size was measured every four days in empty vectors and LINC01311-OE groups. (C) Tumor weight was determined after tumor isolation in LINC01311-OE and empty vector groups. [B and C: $^{**}P < 0.001$ vs. Empty vector; $n = 5$ /group; Student's *t*-test].

was measured. Normalized activity = Firefly Luciferase activity \div Renilla Luciferase activity.

RNA immunoprecipitation (RIP) assay

RNA Immunoprecipitation Kit (Millipore Sigma, USA) was utilized in the detection of LINC01311's interaction with miR-146b-5p. KTC-1 and TPC-1 (4×10^4 cells) were lysed in a 200 μ L harsh lysis buffer. The collected cell lysate was incubated with Protein A Magnetic Beads pre-conjugated with rat anti-IgG or Monoclonal anti-Ago2 antibodies overnight. After that, the magnetic beads were isolated, washed, and digested in a buffer containing Proteinase K. Finally, the RNA was extracted from the immunoprecipitates, and RT-qPCR was applied to analyze the enrichment level of LINC01311 and miR-146b-5p.

In vivo animal experiment

Four to five weeks old BALB/C nude mice (~ 20 g.) were bought from the Center for Animal Experiment/Animal Biosafety Level III laboratory (ABSL-III lab) of Wuhan University (Wuhan, Hubei, China). The *in vivo* tumor models ($n = 5$ /group) were constructed by subcutaneously injecting each mouse with 2×10^3 KTC-1 cells infected with lentiviral particles carrying LINC01311 or empty plasmids. Tumor sizes were monitored once every four days. After 28 days passed, the mice were euthanized by CO₂ inhalation. The xenograft tumors were subsequently excised and weighed. The Institutional Animal Care and Ethics Committee of our hospital granted approval to this animal experiment.

Statistical analysis

Data analysis was performed in GraphPad Prism 9.0 (GraphPad Prism, USA). The data were indicated as mean \pm SD. Data from the two groups were compared by applying a paired student *t*-test. Meanwhile, the differences among multiple groups were tested by One-way ANOVA and Tukey multiple-comparison test. Pearson correlation coefficient was applied to ascertain the correlation of miR-146b-5p with LINC01311 and IMPA2. Lastly, a $P < 0.05$ was indicative of significance.

Results

LINC01311 overexpression suppresses TC cell growth *in vitro* and *in vivo*

We first assessed LINC01311 expression in various TC cell lines. TC cells (KTC-1, BCPAP, TPC-1, and SW579), particularly KTC-1 and TPC-1 cells, expressed lower LINC01311 compared to Nythy-ori3-1 cells (Fig. 1A). We subsequently analyzed the expression of LINC01311 in 28

paired TC and normal tissues and observed a similar downregulation of LINC01311 in TC tissues as well (Fig. 1B). To further characterize the function of LINC01311 in TC cells, we determined its localization within the KTC-1 and TPC-1 cells. The outcomes showed that it is dominantly located in the cytoplasm (Fig. 1C), suggesting its ceRNA activity. To assess the function of LINC01311 in TC cells, we enhanced its expression in the TPC-1 and KTC-1 cells by introducing pCDNA-LINC01311 (LINC01311-OE) into both the cell lines. The results of RT-qPCR analysis revealed that LINC01311 expression was enhanced after the transfection (Fig. 1D). Next, we investigated how LINC01311 overexpression altered TC cell malignant phenotypes such as proliferation, apoptosis, and migration. We found that the proliferative potential of both the TC cell lines was significantly decreased when LINC01311 was overexpressed (Fig. 1E). Furthermore, in KTC-1 and TPC-1 cells overexpressing LINC01311, the relative protein levels of Bax were increased while those of Bcl-2 were decreased, implying that LINC01311 overexpression induces apoptosis (Fig. 1F). Similar results were obtained through flow cytometry, which revealed that overexpression of LINC01311 promoted apoptosis in these cell lines (Fig. 1G). The migratory abilities of both the TC cell lines overexpressing LINC01311 were also reduced as compared to the control cell line (Fig. 1H).

To address whether LINC01311 impacts TC tumorigenesis *in vivo*, we constructed a mouse xenograft tumor model by subcutaneously injecting LINC01311-overexpressing vectors into KTC-1 cells. The results demonstrated that LINC01311 overexpression impeded tumor growth *in vivo* by markedly reducing the size, volume, and weight of the tumors (Fig. 2A-C). Collectively, LINC01311 is an anti-oncogenic lncRNA that suppresses the malignant behavior of TC cells, both *in vivo* and *in vitro*.

LINC01311 targets miR-146b-5p

Next, we investigated for the target miRNA of LINC01311 in order to understand its ceRNA activity in influencing the malignant behaviors of TC cells. Through starBase analysis, we found that LINC01311 preferentially binds with miR-146b-5p (Fig. 3A). Furthermore, the miR-146b-5p mimic decreased the luciferase activity of KTC-1 and TPC-1 cells transfected with LINC01311-WT but did not affect their luciferase activity when transfected with LINC01311-MUT (Fig. 3B). The results of the RIP assay demonstrated that the enrichment of LINC01311 and miR-146b-5p was considerably higher in the Anti-Ago2 group compared to the Anti-IgG group in the KTC-1 and TPC-1 cells, indicating that LINC01311 recognized miR-146b-5p by base pairing (Fig. 3C). Contrary to the poor expression of LINC01311 in TC cells and tissues, miR-146b-5p expression was enhanced in TC cells and tissues (Fig. 3D and E). Furthermore, we observed a negative correlation between the expressions of LINC01311 and miR-146b-5p (Fig. 3F).

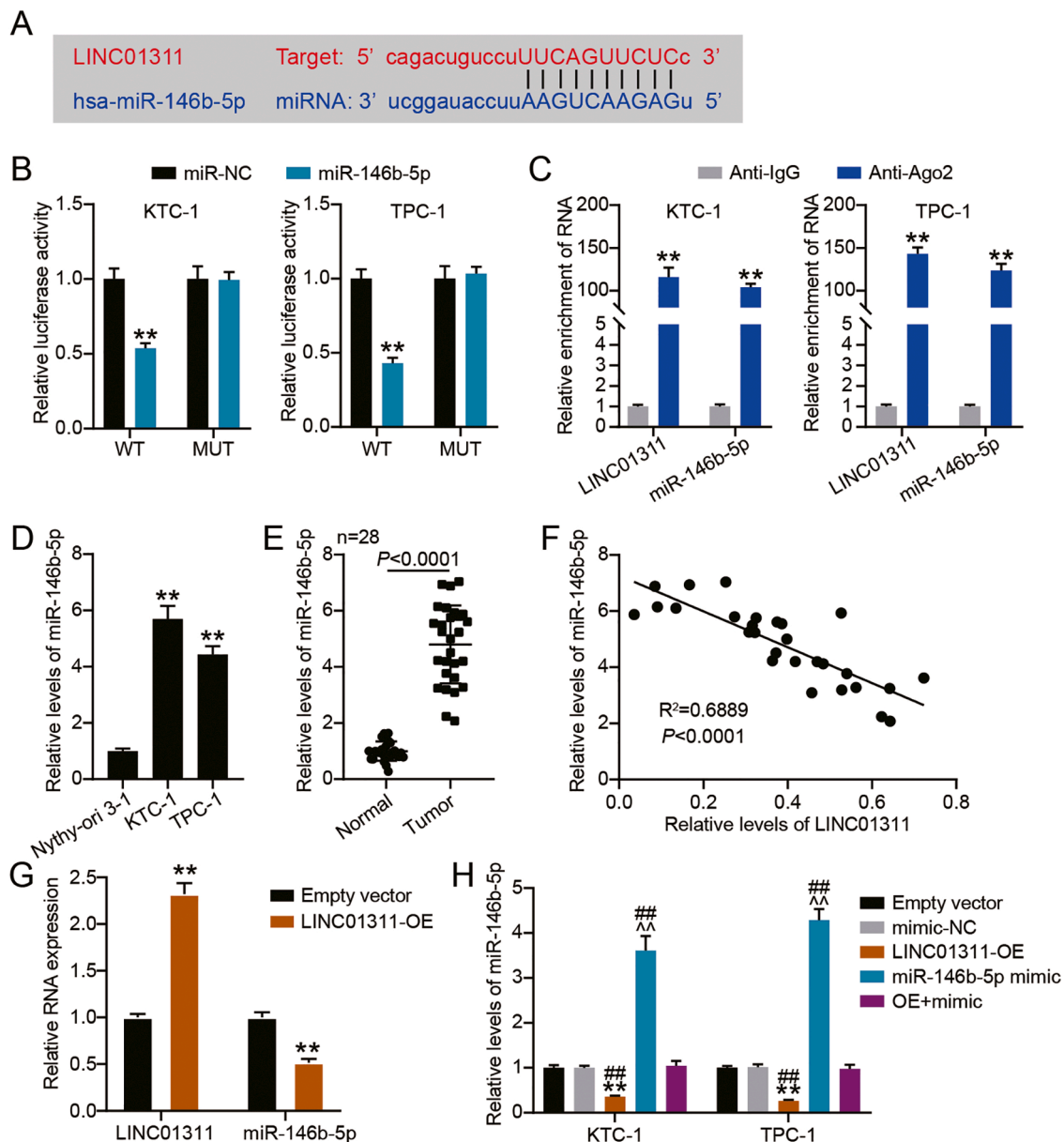


Fig. 3. *LINC0311* targets *miR-146b-5p*. (A) StarBase predicted that *miR-146b-5p* might bind with *LINC0311*. (B) Luciferase activity in extracts from KTC-1 and TPC-1 cells co-transfected with *LINC0311*-WT/MUT luciferase vectors and *miR-146b-5p* mimic or *miR-NC*. [$**P < 0.001$ vs. *miR-NC*; $n = 3$ /group; Student's *t*-test]. (C) Ago2 RNA immunoprecipitation (RIP) assay was performed to detect *miR-146b-5p* and *LINC0311* levels in KTC-1 and TPC-1 cells with Ago2. [$**P < 0.001$ vs. Anti-Ago2; $n = 3$ /group; Student's *t*-test]. (D) RT-qPCR analysis of *miR-146b-5p* in TC cells (KTC-1 and TPC-1) and normal cells (Nythy-ori3-1). [$**P < 0.001$ vs. Nythy-ori3-1; $n = 3$ /group; Dunnett's post hoc test]. (E) RT-qPCR analysis of *miR-146b-5p* in normal and TC tissues. [$**P < 0.0001$ vs. normal tissues; $n = 28$ /group; Welch's *t*-test]. (F) Pearson correlation coefficient indicating the correlation of *LINC0311* expression with that of *miR-146b-5p* in TC tissues. (G) RT-qPCR analysis of *LINC0311* and *miR-146b-5p* expression in xenograft tumors. [$**P < 0.001$ vs. Empty vector; $n = 5$ /group; Student's *t*-test]. (H) *LINC0311* overexpressing vectors (*LINC0311*-OE), Empty vectors, *miR-146b-5p* mimic (mimic), mimic-NC, and *LINC0311*-OE (OE)+mimic were transfected into KTC-1 and TPC-1 cells. Relative *miR-146b-5p* levels in the transfected TC cells were quantified via RT-qPCR analysis. [$**P < 0.001$ vs. Empty vector; $##P < 0.001$ vs. mimic-NC; $^{\sim}P < 0.001$ vs. *LINC0311*-OE (OE)+mimic; $n = 3$ /group; Dunnett's post hoc test].

We then examined the expression of *LINC0311* and *miR146b-5p* in xenograft tumors to confirm the negative connection between the two. The results demonstrated that *LINC0311* expression was elevated whereas *miR-146b-5p* expression was downregulated in tumors overexpressing *LINC0311*, confirming the negative correlation (Fig. 3G). Notably, overexpression of *LINC0311* mitigated the elevated *miR-146b-5p* levels caused by the *miR-146b-5p* mimic in KTC-1 and TPC-1 cells (Fig. 3H). The aforementioned findings suggest that *LINC0311* sponges *miR-146b-5p* to downregulate *miR-146b-5p* expression.

LINC0311 interacts with *miR-146b-5p* to antagonize the anti-oncogenic role of *LINC0311* in TC

To investigate the functionality of the *LINC0311*–*miR-146b-5p* interaction, we studied the alternation of phenotypes in TC cells co-transfected with *LINC0311* overexpressing vectors and *miR-146b-5p* mimic. Intriguingly, a significant rise in cell proliferation was observed in KTC-1 and TPC-1 cells that overexpressed *miR-146b-5p*. This increase in proliferation was nearly negated upon the additional transfection of *LINC0311* overexpressing vector in both the TC cell lines (Fig. 4A). Conversely, the overexpression of *miR-146b-5p* induced

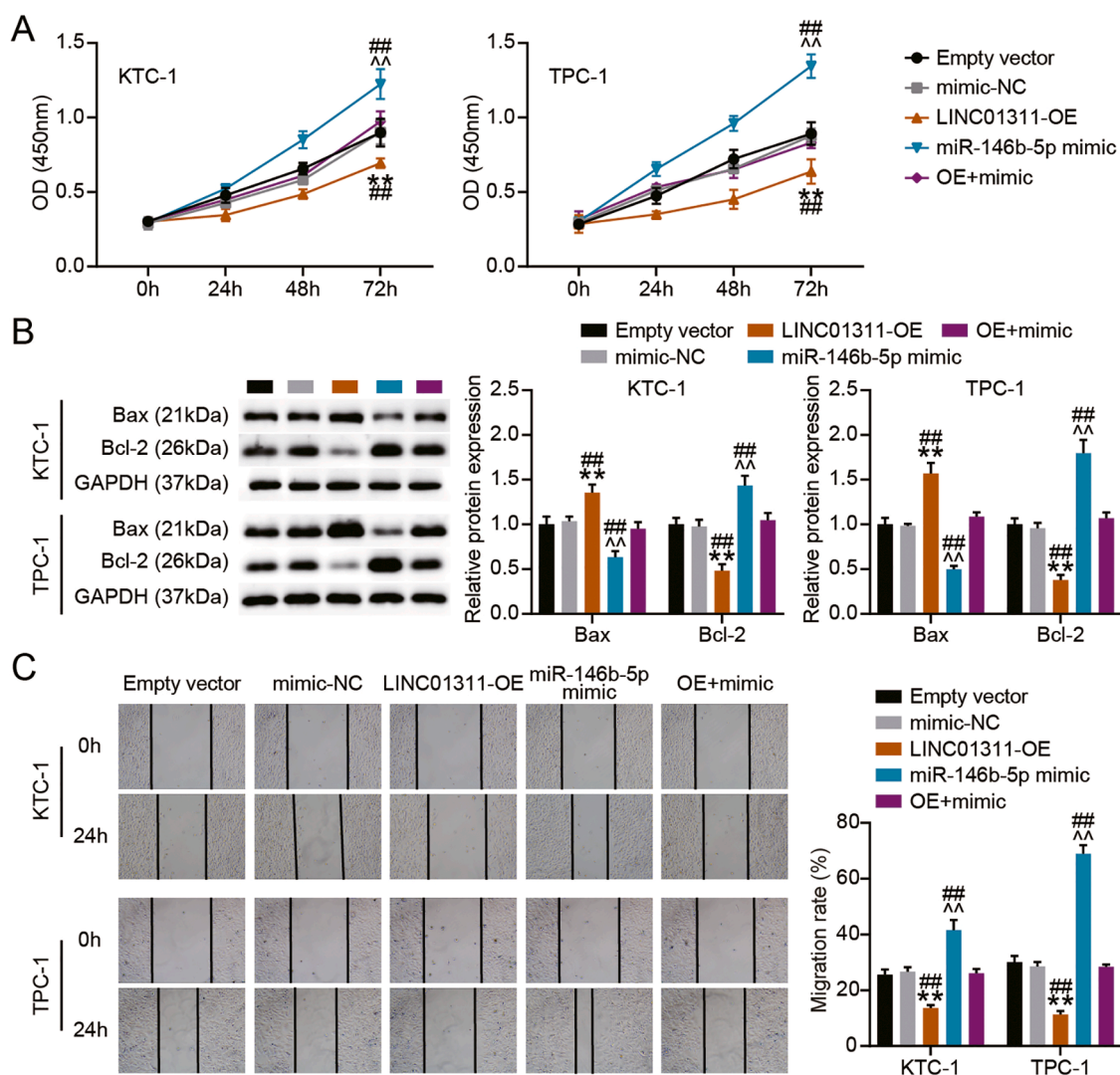


Fig. 4. LINC01311 interacts with miR-146b-5p to counteract the tumor-suppressive role of LINC01311 in TC cells. KTC-1 and TPC-1 cells were transfected with LINC01311 overexpressing vectors (LINC01311-OE), Empty vectors, miR-146b-5p mimic (mimic), mimic-NC, and LINC01311-OE (OE)+mimic. after 48 h. (A) Cell viability in different groups was tested by CCK-8. (B) Western blot analysis of the different groups using anti-Bax and anti-Bcl-2 antibodies. (C) Analysis of tumor cells migration by scratch wound-healing assay in different groups. [^{***} $P < 0.001$ when compared to the Empty vectors; ^{##} $P < 0.001$ when compared to mimic-NC; [^] $P < 0.001$ vs. LINC01311-OE (OE)+mimic; $n = 3$ /group; Dunnett's post hoc test].

by the transfection of the miR-146b-5p mimic constrained TC cell apoptosis. This was demonstrated by elevated Bcl-2 and reduced Bax protein levels in KTC-1 and TPC-1 cells (Fig. 4B). However, this suppression of apoptosis was offset by the overexpression of LINC01311. In scratch wound-healing assays, miR-146b-5p-overexpressing TC cells manifested increased cell migration. Meanwhile, the co-introduction of LINC01311 overexpressing vectors and miR-146b-5p mimic overturned this increase (Fig. 4C). These findings indicate that LINC01311 may directly interact with miR-146b-5p to constrain the malignant behaviors of TC cells.

miR-146b-5p recognizes IMPA2 and downregulates its expression

Next, we attempted to understand the mechanism by which miR-146b-5p promoted cellular proliferation and migration by exploring possible transcription silencing in TC cells with miR-146b-5p overexpression. The starBase prediction showed that miR-146b-5p might target IMPA2 (Fig. 5A). To substantiate this, we performed a luciferase reporter assay and observed that miR-146b-5p mimic could evoke a considerable reduction in the luciferase activity of TC cells transfected with IMPA2-WT while having no effect on the luciferase activity of TC

cells transfected with IMPA2-MUT (Fig. 5B). The result indicated that miR-146b-5p could directly target the 3' UTR of IMPA2. A notable downregulation of IMPA2 was also detected in TC cells and tissues (Fig. 5C and D). In addition, IMPA2 expression was found to be negatively correlated with miR-146b-5p expression TC tissues (Fig. 5E). More importantly, miR-146b-5p mimic offset the overexpression of IMPA2 in TC cells, which was engendered by the transfection of IMPA2 overexpressing vectors (Fig. 5F). Based on the findings presented above, it is reasonable to conclude that miR-146b-5p interferes with IMPA2 expression by binding with its 3'UTR.

IMPA2 overexpression overturns miR-146b-5p's oncogenic activity in TC cells

After determining the direct interaction of miR-146b-5p with the IMPA2 3'UTR, we further investigated whether IMPA2 downregulation is a crucial step for the oncogenic activity of miR-146b-5p. As a result, the ectopic expression of IMPA2 impaired the proliferative capacity of TC cells. This anti-proliferative potential of IMPA2, however, was reversed upon the additional introduction of the miR-146b-5p mimic (Fig. 6A). The outcomes of the western blot experiment performed using

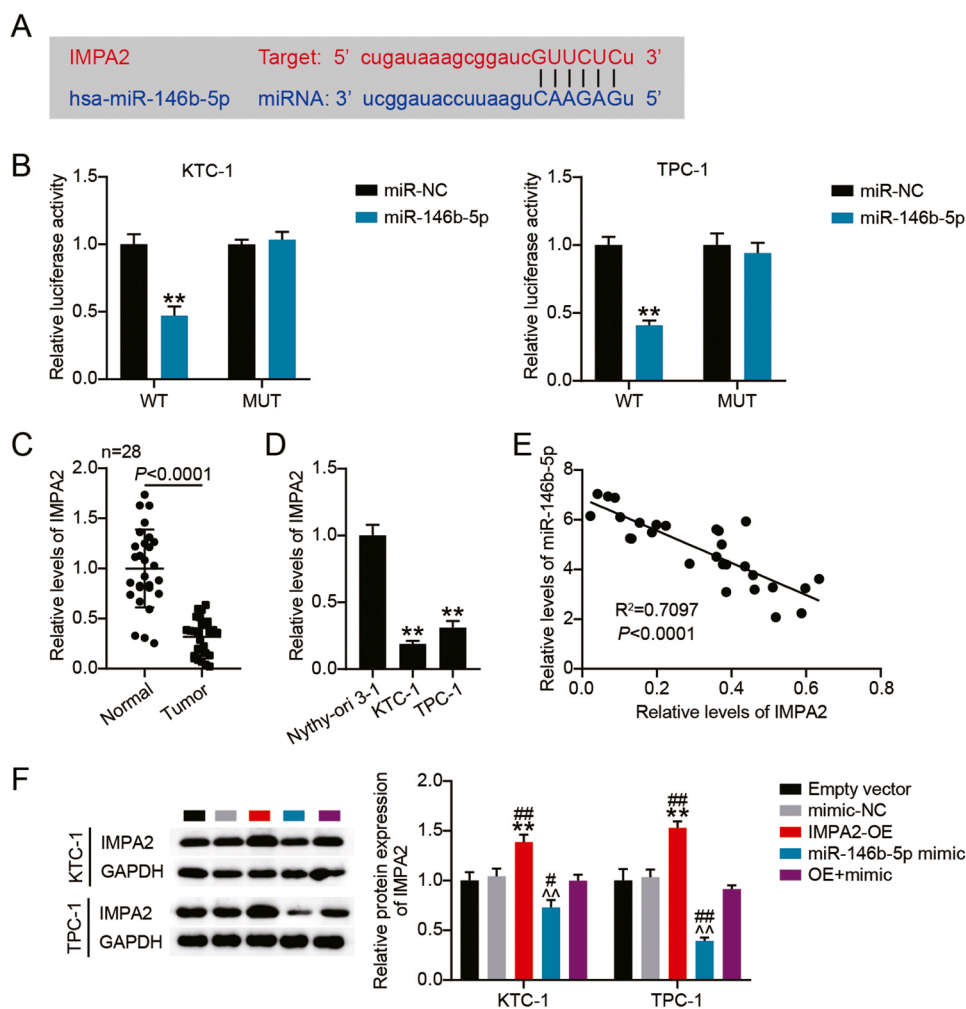


Fig. 5. *MiR-146b-5p* recognizes *IMPA2* and downregulates its expression. (A) The binding sites shared by *miR-146b-5p* and *IMPA2* 3'UTR, as predicted by starBase. (B) Dual-luciferase reporter experiment verified the binding of *IMPA2* 3'UTR with *miR-146b-5p*. [$**P < 0.001$ vs. *miR-NC*; $n = 3$ /group; Student's *t*-test]. (C) RT-qPCR analysis of *IMPA2* expression in TC tissues and normal tissues. [$**P < 0.0001$ vs. normal tissues; $n = 28$ /group; Welch's *t*-test]. (D) RT-qPCR analysis of *IMPA2* expression in TC cells (KTC-1 and TPC-1) and normal cells (Nythy-ori3-1). [$**P < 0.001$ vs. Nythy-ori3-1; $n = 3$ /group; Dunnett's post hoc test]. (E) Pearson correlation coefficient revealed the association of *IMPA2* expression with that of *miR-146b-5p* in TC tissues. (F) KTC-1 and TPC-1 cells were transfected with *miR-146b-5p* mimic (mimic), mimic-NC, Empty vector, *IMPA2* overexpressing vectors (*IMPA2*-OE), and *IMPA2*-OE (OE)+mimic. Western blotting was performed to estimate *IMPA2* expression in the different groups. [$**P < 0.001$ when compared to Empty vector; $##P < 0.001$ when compared to mimic-NC; $^*P < 0.001$ when compared to *IMPA2*-OE (OE)+mimic; $n = 3$ /group; Dunnett's post hoc test].

anti-Bcl-2 and anti-Bax antibodies revealed that *IMPA2*-overexpressing TC cells manifested elevated Bax and reduced Bcl-2 protein expression levels, indicating enhanced apoptosis. This outcome, however, was mitigated by the addition of the *miR-146b-5p* mimic (Fig. 6B). In addition, we observed that *IMPA2* overexpression reduced the migration of TC cells. This anti-migratory action, again, was counteracted by the *miR-146b-5p* mimic (Fig. 6C). These results suggest that the oncogenic role of *miR-146b-5p* may be reliant, at least in part, on the down-regulation of *IMPA2*.

Discussion

In the present work, we found poor expression of LINC01311 in TC cells and tissues, implying that LINC01311 may play a role in TC progression. Furthermore, we found that ectopic expression of LINC01311 reduced the proliferative and migratory potentials of TC cells *in vitro* and triggered apoptosis. This inhibitory effect was also manifested *in vivo*. To the best of our knowledge, our results are the first to demonstrate the tumor-suppressive activity of LINC01311 in cancer. Mechanistically, we further characterized the novel ceRNA activity of LINC01311 wherein it sponged *miR-146b-5p*. This reversed the *miR-146b-5p*-mediated *IMPA2* silencing, thereby suppressing the malignant behaviors of the TC cells. This newly discovered ceRNA regulatory network of LINC01311/*miR-146b-5p*/*IMPA2* establishes the foundation for targeted therapies against TC.

Previously, *miR-146b-5p* has been reported to act as either a tumor promoter or suppressor in different malignancies [17–19]. For example,

miR-146b-5p has been shown to be an oncogenic miRNA in colorectal and papillary thyroid carcinoma *in vitro* and *in vivo* [20,21]. On the contrary, it has been reported to function as a tumor suppressor miRNA in non-small cell lung cancer and T-cell acute lymphoblastic leukemia [19]. We observed elevated *miR-146b-5p* expression in TC cells and tissues and our functional assays demonstrated that the high *miR-146b-5p* levels promoted TC cell migration and proliferation and impeded apoptosis. Hence, our results suggests that *miR-146b-5p* act as an oncogenic miRNA in TC. Our findings are consistent with previous reports that showed *miR-146b-5p* overexpression increased TC cell migration and proliferation [13,14], validating *miR-146b-5p*'s oncogenic function in TC progression. Interestingly, via luciferase reporter and RIP assays, we discovered that *miR-146b-5p* is a target of LINC01311's ceRNA activity. LINC01311 overexpression suppressed the expression of *miR-146b-5p* as well as its oncogenic role, therefore inhibiting the progression of TC. Although other lncRNAs have been reported to target *miR-146b-5p* [19,22–24], our study is the first to reveal the interaction of *miR-146b-5p* with LINC01311, which suggests a novel regulatory mechanism for *miR-146b-5p* modulation.

lncRNAs sequester miRNAs by sponging them and thereby attenuate the repressive effect of miRNAs on mRNAs [25]. Here, we found that *miR-146b-5p* targeted *IMPA2* 3' UTR by our bioinformatics analysis as well as luciferase reporter assay. The *IMPA2* gene is located on chromosome 18p11.21 and consists of 9 exons. This gene encodes an inositol monophosphatase which catalyzes the dephosphorylation of inositol monophosphate and executes a significant role in phosphatidylinositol signaling [26]. In cervical cancer, *IMPA2* expression is reportedly

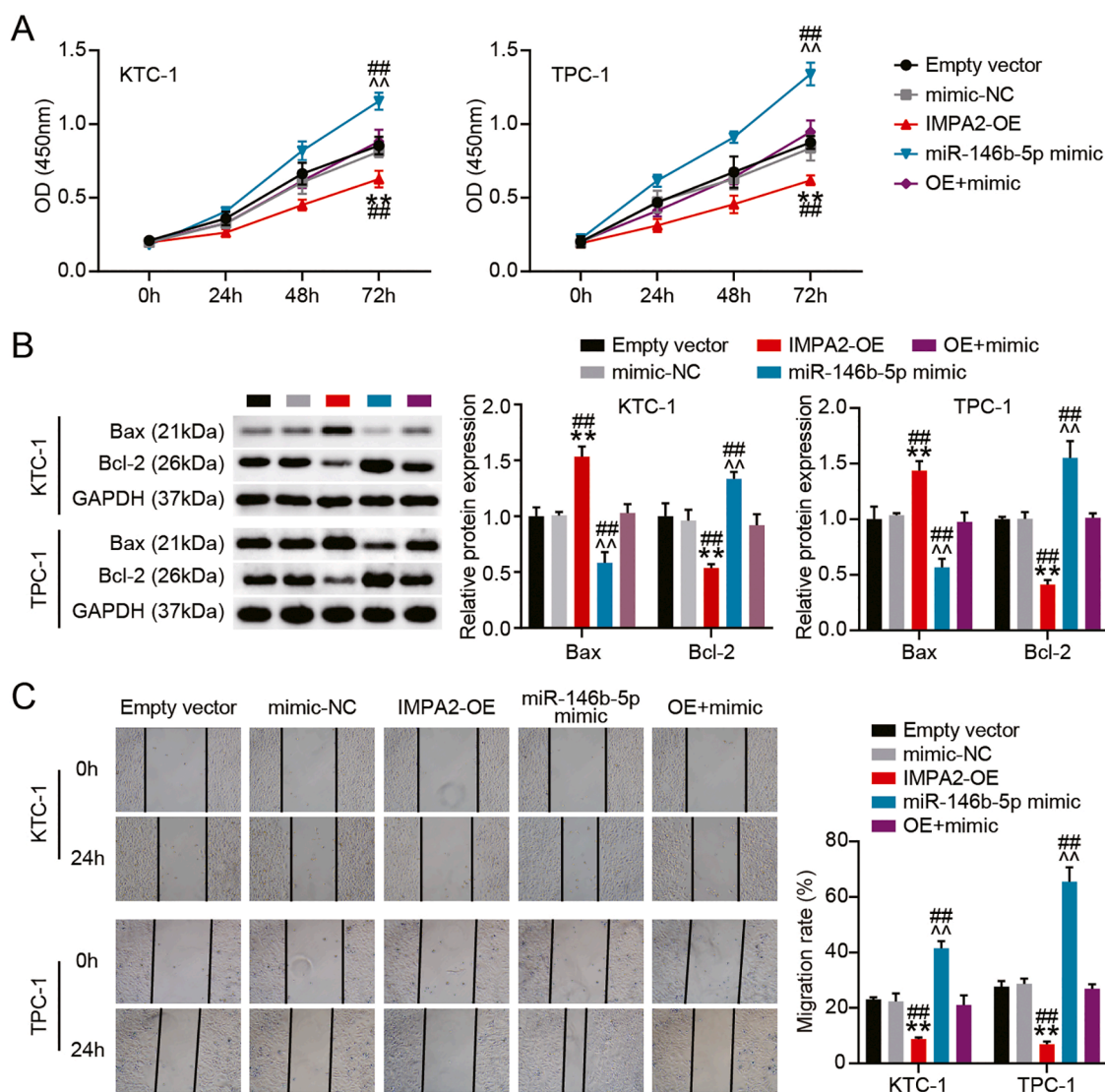


Fig. 6. IMPA2 overexpression counteracts miR-146b-5p's oncogenic action in TC cells. KTC-1 and TPC-1 cells were transfected with miR-146b-5p mimic (mimic), mimic-NC, Empty vector, IMPA2 overexpressing vectors (IMPA2-OE), and IMPA2-OE (OE)+mimic. After 48 h. (A) Cell viability in different groups was tested by CCK-8. (B) Western blot analysis of the different groups using anti-Bax and anti-Bcl-2 antibodies. (C) Analysis of tumor cell migration in the different groups by means of the scratch wound-healing assay. [$**P < 0.001$ vs. Empty vector; $\#P < 0.05$, $\#\#P < 0.001$ vs. mimic-NC; $\#P < 0.001$ vs. IMPA2-OE (OE)+mimic; $n = 3$ /group; Dunnett's post hoc test].

increased in the tumor and the short hairpin RNA (shRNA)-mediated IMPA2 silencing suppressed the malignant potential of tumor cells by attenuating ERK phosphorylation [26]. In clear cell renal cell carcinoma, IMPA2 downregulation is a novel biomarker of dismal prognosis of the tumor, and its silencing has been reported to drive the proliferation of tumor cells [27,28]. In TC, we found reduced expression of IMPA2 in tumors and overexpressing IMPA2 hampered the migration and proliferation of TC cells while boosting apoptosis. We are first to report the tumor-suppressive role of IMPA2 in TC. Furthermore, rescue assays also demonstrated that the miR-146b-5p mimic could offset the IMPA2-overexpression-induced suppression of migration and proliferation as well as the stimulation of apoptosis in TC cells. Our findings provide novel insights on the epigenetic modification of miR-146b-5p during TC progression.

This study has some limitations, and future research is needed to address them. First, the ceRNA regulatory network constituted by LINC01311, miR-146b-5p, and IMPA2 may be more complex due to the different possible targets among them. For example, miR-146b-5p regulates lncRNA MALAT1 expression and drives the progression of TC

[14]. Our future research will concentrate on these complex regulatory networks. Second, some regulatory factors have been reported to play anti-tumor roles in cancers such as granulocyte colony-stimulating factor [29], bruton's tyrosine kinase [30], shikonin [31]. Therefore, we will explore the key anti-tumor factors associated with LINC01311/miR-146b-5p/IMPA2 axis in TC in the future. In addition, the clinical outcome requires additional confirmation with a large sample size, and the downstream effector of IMPA2 needs to be investigated further.

Conclusion

We identified LINC01311 as a tumor suppressor, both *in vitro* and *in vivo*. LINC01311 mitigates TC cell migration and proliferation and promotes apoptosis via sponging miR-146b-5p to upregulate IMPA2 expression. Overall, our research establishes the groundwork for TC intervention.

Declarations

Funding

This study did not receive any funding in any form.

Ethics approval

The present study was approved by the Ethics Committee of Hubei NO.3 People's Hospital of Jiangnan University (Wuhan, China). The processing of clinical tissue samples is in strict compliance with the ethical standards of the Declaration of Helsinki. All patients signed written informed consent.

This animal experiment was conducted in accordance with the ARRIVE guidelines and was authorized by the Institutional Animal Care and Ethics Committee of Hubei NO.3 People's Hospital of Jiangnan University.

Consent to participate

All patients signed a written informed consent.

Consent for publication

Consent for publication was obtained from the participants.

Availability of data and material

All data generated or analyzed during this study are included in this article.

Authors' contributions

MJL and LHZ conducted the experiments and data analysis. JPH and CY conceived and designed the study. YZ and ZDY acquired the data. ZDY and MJL carried out the analysis and interpretation of data. All authors have read and approved this manuscript.

Declaration of Competing Interest

The authors declare that they have no known competing financial interests or personal relationships that could have appeared to influence the work reported in this paper.

Acknowledgments

None.

References

- [1] S. Vaccarella, J. Lortet-Tieulent, M. Colombet, L. Davies, C.A. Stiller, J. Schüz, et al., Global patterns and trends in incidence and mortality of thyroid cancer in children and adolescents: a population-based study, *Lancet Diabetes Endocrinol* 9 (3) (2021) 144–152.
- [2] A.J. Bauer, Pediatric thyroid cancer: genetics, therapeutics and outcome, *Endocrinol. Metab. Clin. N. Am.* 49 (4) (2020) 589–611.
- [3] L. Davies, J.K. Hoang, Thyroid cancer in the USA: current trends and outstanding questions, *Lancet Diabetes Endocrinol.* 9 (1) (2021) 11–12.
- [4] J. Cao, M. Zhang, L. Zhang, J. Lou, F. Zhou, M. Fang, Non-coding RNA in thyroid cancer - Functions and mechanisms, *Cancer Lett.* 496 (2021) 117–126.
- [5] C. Xing, S.G. Sun, Z.Q. Yue, F. Bai, Role of lncRNA LUCAT1 in cancer, *Biomed. Pharmacother.* 134 (2021), 111158.
- [6] M.C. Bridges, A.C. Daulagala, A. Kourtidis, LNCcation: lncRNA localization and function, *J. Cell Biol.* 220 (2) (2021), e202009045.
- [7] Y.T. Tan, J.F. Lin, T. Li, J.J. Li, R.H. Xu, H.Q. Ju, lncRNA-mediated posttranslational modifications and reprogramming of energy metabolism in cancer, *Cancer Commun.* 41 (2) (2021) 109–120 (London, England).
- [8] H. Liu, H. Deng, Y. Zhao, C. Li, Y. Liang, lncRNA XIST/miR-34a axis modulates the cell proliferation and tumor growth of thyroid cancer through MET-PI3K-AKT signaling, *J. Exp. Clin. Cancer Res. CR* 37 (1) (2018) 279.
- [9] H. Lei, Y. Gao, X. Xu, lncRNA TUG1 influences papillary thyroid cancer cell proliferation, migration and EMT formation through targeting miR-145, *Acta Biochim. Biophys. Sin.* 49 (7) (2017) 588–597 (Shanghai).
- [10] M. Ye, S. Dong, H. Hou, T. Zhang, M. Shen, Oncogenic role of long noncoding RNAMALAT1 in thyroid cancer progression through regulation of the miR-204/IGF2BP2/m6A-MYC signaling, *Mol. Ther. Nucl. Acids* 23 (2021) 1–12.
- [11] Y. Fan, J. Zhang, X. Zhuang, F. Geng, G. Jiang, X. Yang, Epigenetic transcripts of LINC01311 and hsa-miR-146a-5p regulate neural development in a cellular model of Alzheimer's disease, *IUBMB Life* 73 (7) (2021) 916–926.
- [12] X. Qi, D.H. Zhang, N. Wu, J.H. Xiao, X. Wang, W. Ma, ceRNA in cancer: possible functions and clinical implications, *J. Med. Genet.* 52 (10) (2015) 710–718.
- [13] Y. Pan, W. Yun, B. Shi, R. Cui, C. Liu, Z. Ding, et al., Downregulation of miR-146b-5p via iodine involvement repressed papillary thyroid carcinoma cell proliferation, *J. Mol. Endocrinol.* 65 (2) (2020) 1–10.
- [14] Y. Peng, X. Fang, H. Yao, Y. Zhang, J. Shi, MiR-146b-5p regulates the expression of long noncoding RNA MALAT1 and its effect on the invasion and proliferation of papillary thyroid cancer, *Cancer Biother. Radiopharm.* 36 (5) (2021) 433–440.
- [15] K. Jiang, G. Li, W. Chen, L. Song, T. Wei, Z. Li, et al., Plasma exosomal miR-146b-5p and miR-222-3p are potential biomarkers for lymph node metastasis in papillary thyroid carcinomas, *Oncotargets Ther.* 13 (2020) 1311–1319.
- [16] X. Deng, B. Wu, K. Xiao, J. Kang, J. Xie, X. Zhang, et al., MiR-146b-5p promotes metastasis and induces epithelial-mesenchymal transition in thyroid cancer by targeting ZNF3, *Cell. Physiol. Biochem.* 35 (1) (2015) 71–82, international journal of experimental cellular physiology, biochemistry, and pharmacology.
- [17] H. Wang, L. Tan, X. Dong, L. Liu, Q. Jiang, H. Li, et al., MiR-146b-5p suppresses the malignancy of GSC/MSC fusion cells by targeting SMARCA5, *Aging* 12 (13) (2020) 13647–13667.
- [18] Y. Li, H. Zhang, Y. Dong, Y. Fan, Y. Li, C. Zhao, et al., MiR-146b-5p functions as a suppressor miRNA and prognosis predictor in non-small cell lung cancer, *J. Cancer* 8 (9) (2017) 1704–1716.
- [19] Y.Y. Luo, Z.H. Wang, Q. Yu, L.L. Yuan, H.L. Peng, Y.X. Xu, lncRNA-NEAT1 promotes proliferation of T-ALL cells via miR-146b-5p/NOTCH1 signaling pathway, *Pathol. Res. Pract.* 216 (11) (2020), 153212.
- [20] Y. Zhu, G. Wu, W. Yan, H. Zhan, P. Sun, miR-146b-5p regulates cell growth, invasion, and metabolism by targeting PDHB in colorectal cancer, *Am. J. Cancer Res.* 7 (5) (2017) 1136–1150.
- [21] M. Jia, Y. Shi, Z. Li, X. Lu, J. Wang, MicroRNA-146b-5p as an oncomiR promotes papillary thyroid carcinoma development by targeting CCD6, *Cancer Lett.* 443 (2019) 145–156.
- [22] J. Zhou, M. Liu, Y. Chen, S. Xu, Y. Guo, L. Zhao, Cucurbitacin B suppresses proliferation of pancreatic cancer cells by ceRNA: effect of miR-146b-5p and lncRNA-AFAP1-AS1, *J. Cell. Physiol.* 234 (4) (2019) 4655–4667.
- [23] E. Zhang, X. Li, lncRNA SOX2-OT regulates proliferation and metastasis of nasopharyngeal carcinoma cells through miR-146b-5p/HNRNPA2B1 pathway, *J. Cell. Biochem.* 120 (10) (2019) 16575–16588.
- [24] S. Li, J. Hao, Y. Hong, J. Mai, W. Huang, Long Non-coding RNA NEAT1 promotes the proliferation, migration, and metastasis of human breast-cancer cells by inhibiting miR-146b-5p expression, *Cancer Manag. Res.* 12 (2020) 6091–6101.
- [25] L. Salmena, L. Poliseno, Y. Tay, L. Kats, P.P. Pandolfi, A ceRNA hypothesis: the Rosetta stone of a hidden RNA language? *Cell* 146 (3) (2011) 353–358.
- [26] K. Zhang, L. Liu, M. Wang, M. Yang, X. Li, X. Xia, et al., A novel function of IMPA2, plays a tumor-promoting role in cervical cancer, *Cell Death. Dis.* 11 (5) (2020) 371.
- [27] C.H. Kuei, H.Y. Lin, H.H. Lee, C.H. Lin, J.Q. Zheng, K.C. Chen, et al., IMPA2 downregulation enhances mTORC1 activity and restrains autophagy initiation in metastatic clear cell renal cell carcinoma, *J. Clin. Med.* 9 (4) (2020).
- [28] Y.F. Lin, J.L. Chou, J.S. Chang, I.J. Chiu, H.W. Chiu, Y.F. Lin, Dysregulation of the miR-25-IMPA2 axis promotes metastatic progression in clear cell renal cell carcinoma, *EBioMedicine* 45 (2019) 220–230.
- [29] P. Dwivedi, K.D. Greis, Granulocyte colony-stimulating factor receptor signaling in severe congenital neutropenia, chronic neutrophilic leukemia, and related malignancies, *Exp. Hematol.* 46 (2017) 9–20.
- [30] P. Dwivedi, D.E. Muench, M. Wagner, M. Azam, H.L. Grimes, K.D. Greis, Time resolved quantitative phospho-tyrosine analysis reveals Bruton's Tyrosine kinase mediated signaling downstream of the mutated granulocyte-colony stimulating factor receptors, *Leukemia* 33 (1) (2019) 75–87.
- [31] P. Dwivedi, ROS mediated apoptotic pathways in primary effusion lymphoma: comment on induction of apoptosis by Shikonin through ROS-mediated intrinsic and extrinsic pathways in primary effusion lymphoma, *Transl. Oncol.* 14 (7) (2021), 101061.